Third International Conference on Sustainable Construction Materials and Technologies http://www.claisse.info/Proceedings.htm

Investigation of the Cause of Reinforcing Steel Fracture Induced by Alkali-Silica Reaction and Study on Maintenance

Kazunori Sasaki[1], Misa Fujibayashi[2], Masakazu Tona[3], Akinori Sato[4], Yoshio Hisari[5] and Toyoaki Miyagawa[6]

[1]*Osaka Construction Dept., Construction Management Headquarters, Hanshin Expressway Company Limited, 1-2-1-1900 Benten, Minato-ku, Osaka 552-0007, Japan. kazunori-sasaki@hanshin-exp.co.jp*
[2]*Osaka Business & Maintenance Dept., Hanshin Expressway Company Limited, 3-1-25 Ishida, Minato-ku, Osaka 552-0006, Japan. misa-fujibayashi@hanshin-exp.co.jp*
[3]*Osaka Business & Maintenance Dept., Hanshin Expressway Company Limited, 2-11-12 Kosei, Minato-ku, Osaka 552-0023, Japan. masakazu-tona@hanshin-exp.co.jp*
[4]*Sakai Construction Dept., Construction Management Headquarters, Hanshin Expressway Company Limited, 2-3-20 Minami-Hanadaguchicho, Sakai-ku, Sakai 590-0075, Japan. akinori-sato@hanshin-exp.co.jp*
[5]*Planning and Investigation Division, Hanshin Expressway Management Technology Center, 4-5-7, Minami Honmachi, Chuo-ku, Osaka 541-0054, Japan. hisari@tech-center.or.jp*
[6]*Dept. of Civil & Earth Resources Eng., Kyoto University, Nishikyo, Kyoto 615-8540, Japan. miyagawa@sme.kuciv.kyoto-u.ac.jp*

ABSTRACT

There are an increasing number of reports of reinforcing steels fractured or cracked at the bend with the progress of alkali-silica reaction-induced deterioration in old structures. This study investigated the cause of reinforcing steel fracture, with the focus placed on material properties of reinforcing steels, stress as external force and hydrogen embrittlement. The reinforcing steel fracture was likely to occur by the following mechanism: (1) tensile residual stress occurs in the inside of the bend of reinforcing steels due to bending, initiating cracks depending on the rib shape or bending radius; (2) fracture toughness decreases with work hardening or strain aging; (3) corrosion of reinforcing steels causes occlusion of diffusible hydrogen, increasing the risk of hydrogen embrittlement; and (4) cracks propagate due to alkali-silica reaction-induced expansion and tensile residual stress, ultimately causing fracture of reinforcing steels. This paper also includes proposals on maintenance of structures with a risk of reinforcing steel fracture.

Keywords. Alkali-silica reaction, Fracture of reinforcing steel, Residual stress, Fracture toughness value, Hydrogen embrittlement cracking

1. INTRODUCTION

Cracks in concrete attributable to alkali-silica reaction (hereinafter referred to as “ASR”) were found in T-shaped reinforced concrete piers on the Hanshin Expressway in Japan in 1982. A study committee was formed immediately to investigate the cause and countermeasures of ASR-induced cracks which were then almost unknown. They established maintenance guidelines and focused their efforts on controlling the progress of deterioration and understanding the behavior of affected structures through follow-up inspections. Since fracture of reinforcing steels was found in severely deteriorated bridge piers in 2000, more efforts have been made in light of the urgency of the issue to determine the cause of the problem and carry out repair and strengthening work. However, there have been similar reports of reinforcing steel fracture to date. It is highly likely that fractured reinforcing steels remain undetected in structures which were constructed at similar time to or in the same project with those already found to have the problem. This possibility should be taken into account in a new maintenance concept.

The purpose of this study is to determine the cause of ASR-induced fracture of reinforcing steels and present some proposals on maintenance. With the focus placed on materials, external force (stress) and environment, the authors investigated the following subjects: (1) fracture of reinforcing steels; (2) effects of bending on the material properties of reinforcing steels; (3) effects of residual stress in reinforcing steels from bending, as well as effects of ASR-induced expansion force; and (4) possibility of hydrogen embrittlement cracking in reinforcing steels due to deterioration of concrete. The mechanism of reinforcing steel fracture was estimated based on the investigation results. Moreover, proposals were made on maintenance of the structures with a risk of reinforcing steel fracture, including recommendations on selection of structures to be monitored and inspection and examination on them.

2. REINFORCING STEELS FRACTURED DUE TO ASR

Characteristics of reinforcing steels fractured due to ASR are summarized below.

2.1 Appearance. Figure 1 shows a typical example of fractured stirrup. This sample had corrosion in the bent section, being corroded more severely in the inside than in the outside of the bend. Three ribs were found crushed on the inside of the bend, and corrosion was in the vicinity of the crushed ribs. It was likely that these ribs had been crushed during the bending process. Cracks initiated at the bases of the ribs on the inside of the bend.

2.2 Chemical Composition. Table 1 shows the chemical composition analysis results. The values shown in the table are the mean values of fractured reinforcing steel samples taken from an existing pier on the Hanshin Expressway, example values from an existing structure on the Noto Toll Road (Tarui and Torii, 2010), and measurements of two reinforcing steels manufactured in 1980s (Toyohuku, et al., 1988). All of these reinforcing steels were assumed to be SD295A or SD295B of JIS G 3112 steel bars for concrete reinforcement and were found satisfying the specification values. Contents of Cu, Ni, Cr and N which were not specified in the specifications were higher in these samples as compared to blast furnace steel bars. From the similarity in the chemical composition with the electric furnace steel bars of 1980s, the fractured steel samples from the existing road structures were considered to be electric furnace steel bars.

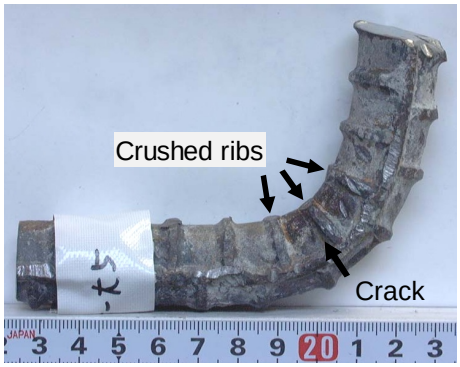

Figure 1. An Example of Appearance of Fractured Reinforcing Steel

Table 1. Chemical Composition Analysis Results (Mass %)

	C	Si	Mn	P	S	Cu	Ni	Cr	N
Hanshin Expressway, average	0.27	0.25	0.77	0.029	0.029	0.31	0.11	0.14	0.0109
Noto Toll Road, example (D32)	0.28	0.18	0.73	0.018	0.026	0.45	0.10	0.18	0.0103
Electric furnace steel bar of 1980s	0.25	0.18	0.90	0.028	0.032	0.31	0.08	0.14	0.0109
Blast furnace steel bar of 1980s	0.25	0.29	1.39	0.029	0.025	0.01	0.02	0.03	0.0042
JIS G 3112 SD295A	–	–	–	≤0.050	≤0.050	–	–	–	–
JIS G 3112 SD295B	≤0.27	≤0.55	≤1.50	≤0.040	≤0.040	–	–	–	–

2.3 Shape of Ribs of Reinforcing Steels. Specifications of the inner radius of the bend (hereinafter referred to as "bending radius") in the JIS G 3112 vary depending on the diameter of reinforcing steel: for instance, at least 1.5 times the nominal diameter for D16 or at least two times the nominal diameter for D22. However, some samples were found to have as small bending radii as 1.2d (d = nominal diameter), and all of them had cracks in the inside of the bend.

Figure 2 shows examples from the rib shape measurement. Although the rib spacing and height were satisfying the JIS G 3112 requirements, there were significant variations in the radius of base curvature of the ribs. The values tended to be smaller on the fractured reinforcing steels as compared to the currently marketed products. In the shown examples, it was 2.85 mm (5.7 mm in diameter) and 3.3 mm (6.6 mm in diameter) on a fractured reinforcing steel (D22), while being 7.85 mm (15.7 mm in diameter) on a product currently on the market (D22). No exact numbers are specified for the radius of base curvature of the ribs in the JIS G 3112 which only requires the rib base to have a shape which allows less concentration of stress.

2.4 Work Hardening (Vickers Hardness). Figure 3 shows Vickers hardness measurement results at the bend and the straight part of reinforcing steels. The inside and outside hardness values were about 40 to 60 (HV10) higher than those at the center of the bend or about 90 (HV10) higher than those in the straight part, showing increases due to the work hardening. According to the approximate conversions between Vickers hardness and tensile strength (Japanese Standards Association, 2009), Vickers hardness values of 240 to

260 (HV10) on the inside and outside of the bend were assumed to be equivalent to tensile strengths of 765 to 825 N/mm^2.

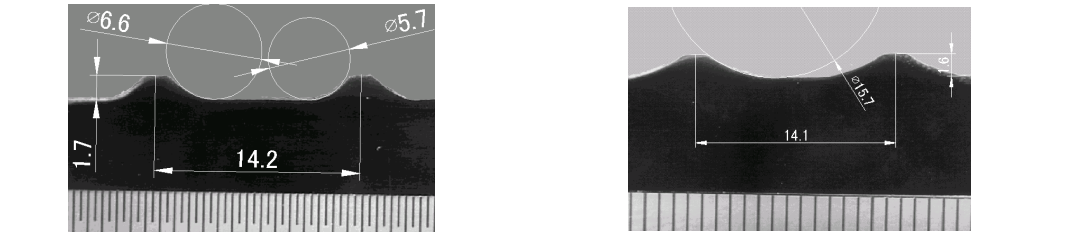

(a) Example of fractured reinforcing steel (D22) (b) Example of currently marketed product (D22)

Figure 2. Rib Shape Measurement Results

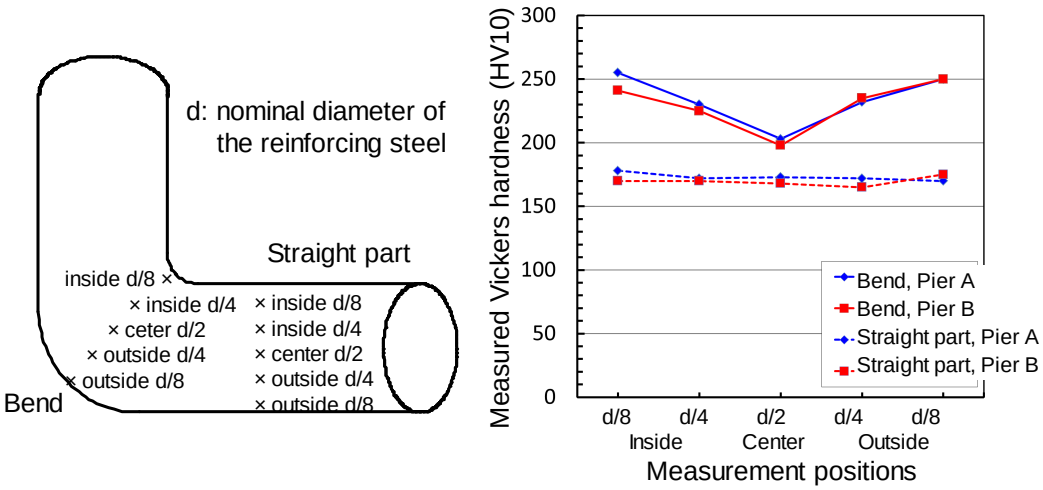

Figure 3. Vickers Hardness Measurement Results

2.5 Properties of Fracture Surface. Figure 4 shows a macro view of the fracture surface of a fractured reinforcing steel. The flat and granular fracture surface with very little plastic deformation suggests a brittle fracture. Cracks initiated at the base of rib on the inside of the bend and, as shown by the radial patterns on the surface, propagated toward the outside of the bend. Minor shear lip was observed at the end point of fracture on the outer periphery. Figure 5 shows the fracture surface observation results by a scanning electron microscope. Cleavage or quasi-cleavage cracks were predominant in the crack propagation region starting from the crack initiating point as shown in Figure 5-(a). Cleavage cracks were predominant in a region about 12 mm inside the crack initiating point as shown in Figure 5-(b). Figure 5-(c) shows the region of shear lip at the crack end point. The elongated dimples in the surface are characteristic to ductile fracture, suggesting a failure by shear.

3. FRACTURE TOUGHNESS VALUE OF REINFORCING STEEL

Work hardening or strain aging in the bent section may lead to toughness reduction in the reinforcing steel. If cracks are present, it is highly likely that resistance against fracture is much affected. The authors investigated the fracture toughness value of fractured reinforcing steels. Samples for the determination of fracture toughness in the bend must be taken from the bent section of the reinforcing steels. However, required samples were not available from

appropriate portions. Instead, samples of the bend were prepared by using samples from the straight part and introducing compressive strain in them to reproduce the strain occurring in the inside of the bend, thereby simulating the effect of the bending process. Fracture toughness test was carried using the specimens taken from these samples.

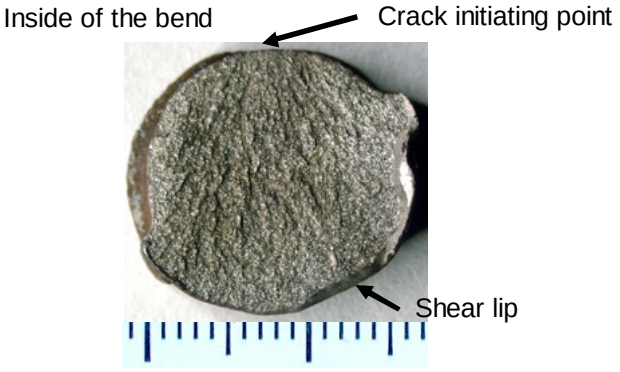

Figure 4. Macro View of Fracture Surface of Fractured Reinforcing Steel (D16)

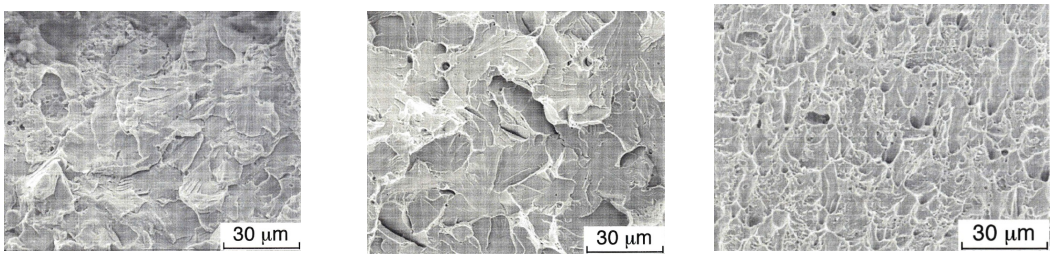

(a) Fracture surface near the crack initiating point

(b) Fracture surface about 12 mm inside

(c) Fracture surface at the shear lip region

Figure 5. Fracture Surfaces of Fractured Reinforcing Steel

3.1 Samples. The test samples were fractured primary reinforcing steels of D32 taken from a beam of an existing reinforced concrete bridge pier (hereinafter referred to as "fractured reinforcing steels"). Control samples for comparison were standard reinforcing steels complying with the current JIS requirements (hereinafter referred to as "JIS-complying reinforcing steels"). The samples were confirmed to have required chemical composition of JIS G 3112 steel bars for concrete reinforcement, satisfying all specification values. Table 2 shows the descriptions of the samples.

3.2 Test Method. Fracture toughness test was carried out at a room temperature (20°C) in compliance with ASTM E1820 [Elastic-Plastic Fracture Toughness (J_{IC}) Testing, Standard Test Method for Measurement of Fracture Toughness]. The J value for stable ductile crack growth was determined by using an electro-hydraulic servo fatigue tester with a maximum capacity of 50 kN. The unloading compliance method was used to determine J values for stable ductile crack growth (J_Q). Details of the test method are not shown here due to the page limit.

3.3 Test Results. Figure 6 shows the relationship between the fracture toughness value and the amount of pre-strain in the fractured reinforcing steels and the JIS-complying reinforcing steels. In the cases with no pre-strain (unprocessed) the JIS-complying reinforcing steel

exhibited a higher value than that of the fractured reinforcing steel. The fracture toughness value decreased significantly in the both reinforcing steels with the introduction of compressive strain simulating the strain in the bend. These results suggest that fracture toughness value at the bend decreases due to work hardening, and that resistance against fracture may be much affected if cracks are present.

Table 2. Test and Control Samples

Locations represented	Reinforcing steel sample types	Specimen symbols	Hardness (HV10)	Amount of strain introduced
Straight part (unprocessed)	Fractured	F-1	170 equivalent	0%
	JIS-complying	S-1	170 equivalent	0%
Bend (processed)	Fractured	F-2	250 equivalent	20.8% compression
	JIS-complying	S-2	250 equivalent	20% compression

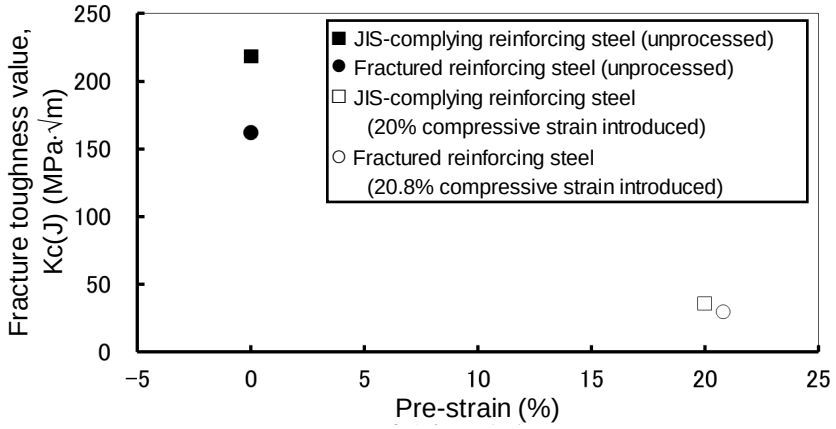

Figure 6. Fracture Toughness Values versus Pre-strain Amounts

4. STRESS IN REINFORCING STEEL

Residual stress from bending and stress from ASR-induced concrete expansion were estimated to understand the change in stress in the reinforcing steels and investigate its effect on the initiation and propagation of cracks.

4.1 Residual Stress in the Bend of Reinforcing Steel. Stress occurring in the reinforcing steel was determined by FEM analysis simulating the bending process with a steel bender. The change in stress during bending was understood as residual stress. The analysis took into account the spring back phenomenon or elastic strain recovery after the removal of confinement at the completion of bending on the reinforcing steel.

Elastic-plastic finite element analysis was adopted in this study, using the analysis application of Abaqus/Standard version 6.5-3.

Reinforcing steel of D16 was modeled into a symmetrical model about the center of bending, using about 23,000 trilinear hexahedral elements. Bending radius was 1d (d = nominal diameter), and the properties of the reinforcing steels were as follows: Young's modulus = 210 GPa; Poisson's ratio = 0.3; and yield stress = 305 MPa.

Figure 7 shows an example of axial stress distribution in a reinforcing steel at the completion

of bending. Compressive stress occurred in the inside of the bend from the center of the cross section, and tensile stress occurred in the outside of the bend. Figure 8 shows an example of axial stress distribution after complete release of the load. The tensile stress regions in the outside of the bend almost disappeared, and tensile stress occurred in the inside surface layer of the bend.

Axial stress showed a general change from tensile stress to compressive stress in the outside of the bend, and a change from compressive stress to tensile stress in the inside surface layer of the bend during the period from completion of bending to complete release of the load. Tensile residual stress of about 300 MPa remained at the rib base, which was considered to be the cause of crack initiation and propagation.

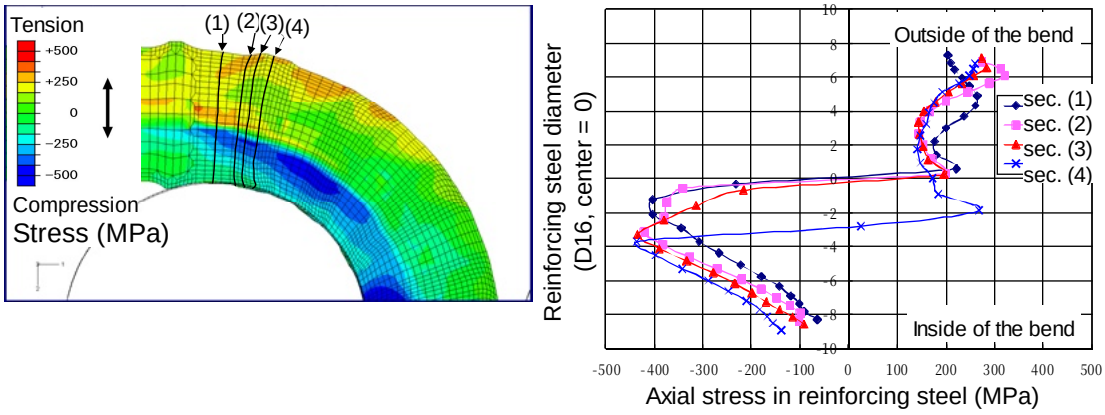

(a) Stress contour diagram (b) Stress distribution

Figure 7. Axial Stress in Reinforcing Steel at the Completion of Bending Process

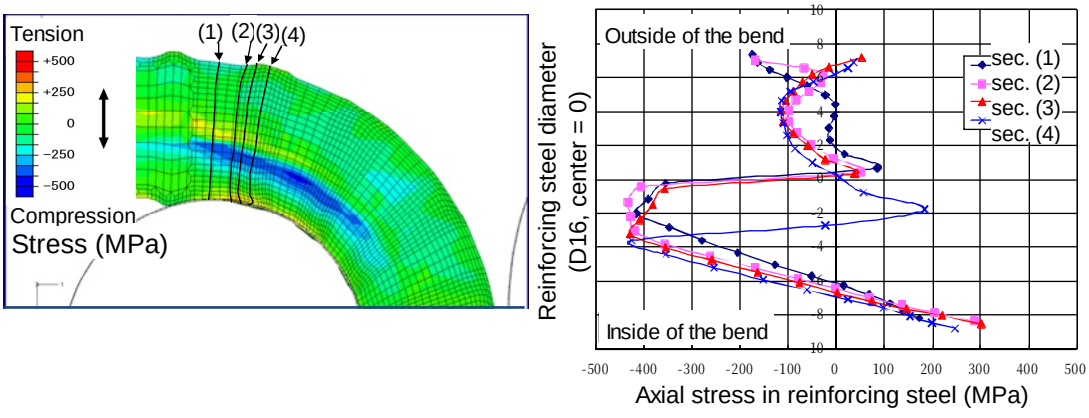

(a) Stress contour diagram (b) Stress distribution

Figure 8. Axial Stress in Reinforcing Steel after Complete Release of the Load

4.2 Stress in Reinforcing Steel Induced by Concrete Expansion. Stress in reinforcing steels induced by concrete expansion was estimated using strain values in reinforcing steels in concrete specimens prepared. Deterioration in an actual bridge pier was successfully reproduced in these specimens through outdoor exposure.

The specimens were prestressed concrete beams of 750×750×5000 mm. Weldable strain gauges were attached to shear reinforcing steels for measurement. Strain exceeded 15,000μ in

the middle part on 900 days (Sasaki et al., 2009). Stress corresponding to the strain of 15,000μ was estimated from the stress-strain curves of the shear reinforcing steels used. The estimation revealed that stress in some reinforcing steels could have reached a yield stress level of 350 MPa. These results suggest that actual stress including residual stress may be extremely high in reinforcing steels.

5. HYDROGEN EMBRITTLEMENT OF REINFORCING STEEL

Hydrogen embrittlement cracking is likely to be one of the causes of reinforcing steel fracture induced by ASR. Since the major causal factor of hydrogen embrittlement is diffusible hydrogen, analysis of hydrogen absorbed in steel is extremely important to discuss the possibility of hydrogen embrittlement. The authors investigated the amount of diffusible hydrogen occluded in reinforcing steels in ASR-damaged concrete and determined the possibility of hydrogen embrittlement cracking from the relationship between the tensile strength of steel and the amount of diffusible hydrogen occluded in the steel.

5.1 Occluded Hydrogen. Samples of bent sections were taken from three stirrups in an existing bridge pier constructed 35 years ago, and occluded hydrogen was measured using an atmospheric pressure ionization-mass spectrometer (API-MS). Figure 9 shows a comparison with separate measurement results on concrete specimens. It was revealed that more diffusible hydrogen was occluded in the inside and outside of the bend than at the center of the bend. About 0.4 ppm of occluded hydrogen was present in the specimen with heavier corrosion. The dependence of the amount of occluded hydrogen on the degree of corrosion was similar in pattern between the existing pier and the concrete specimens in the separate measurement, with more occluded hydrogen present in reinforcing steels with more severe corrosion.

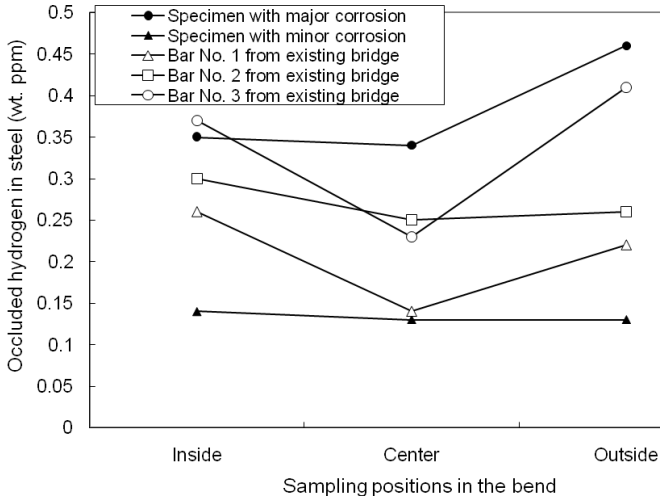

Figure 9. Comparison of Diffusible Hydrogen Occluded in Reinforcing Steels between the Test Specimens and Existing Bridge Pier

5.2 Possibility of Hydrogen Embrittlement. Risk of hydrogen embrittlement cracking was evaluated in the relationship between the steel strength and environmental severity (Figure 10), using the measured amounts of occluded hydrogen in the reinforcing steels and the tensile strength values in cracking regions calculated from the hardness measurement results. All reinforcing steel types in this study were found to fall on the border between the

safe and unacceptable zones. Kobayashi et al. (2010) investigated the possibility of hydrogen embrittlement cracking in reinforcing steels by experiment. In their examination on the effects of strain rate and hydrogen charging current on embrittlement cracking, embrittlement was recognized even with a slight amount of hydrogen charging current when strain rate was adequately slow in the simulated environment of ASR-damaged concrete during the slow strain rate tensile test. This suggests the possibility that embrittlement may occur in the presence of an extremely small amount of hydrogen generation which accompanies corrosion reaction, when strain rate is as slow as that in ASR expansion. Consequently, it is highly possible that hydrogen embrittlement was involved in the fracture of reinforcing steels.

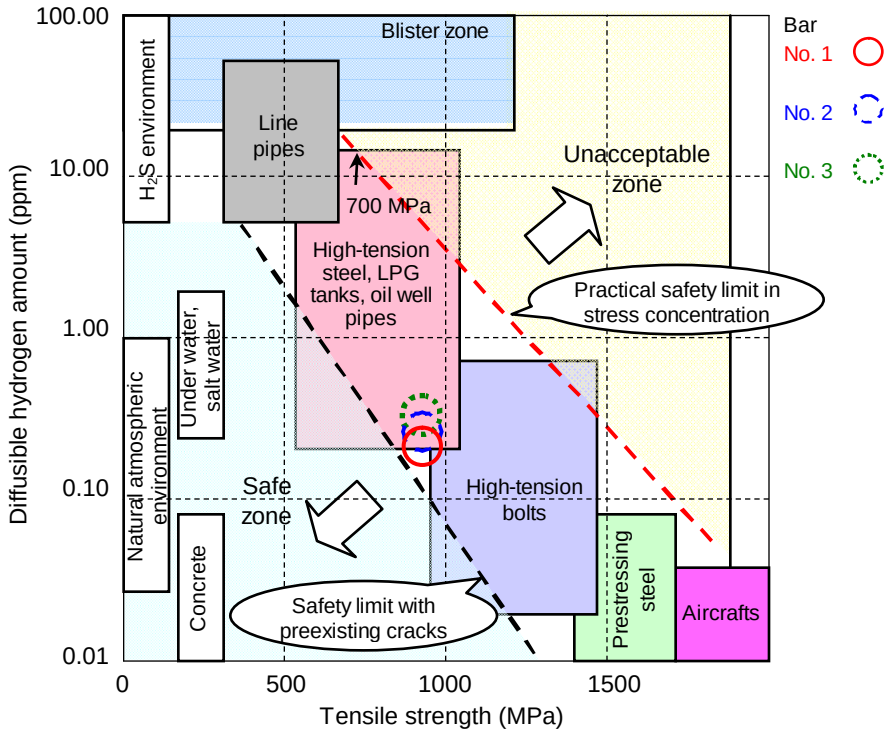

Figure 10. Risk of Hydrogen Embrittlement Cracking in the Relationship between the Steel Strength and Environmental Severity (Matsuyama, 1989)

6. MECHANISM OF ASR-INDUCED REINFORCING STEEL FRACTURE

Reinforcing steel fracture induced by ASR was considered to occur by the mechanism described in Figure 11.

7. PROPOSALS ON MAINTENANCE

Fracture of reinforcing steels induced by ASR affects the load carrying performance of a structure. Therefore, early detection of reinforcing steel fracture is essential to proper maintenance of ASR-affected structures. Selection of structures with a risk of reinforcing steel fracture basically requires understanding of the characteristics in appearance degradation or other changes over time. It is also important to inspect other sections or structures constructed at similar time to or in the same project with those already found affected. Non-destructive testing is recommended for the diagnosis of reinforcing steel fracture. Technological development is expected to improve the precision and accuracy of

non-destructive testing techniques. In consideration of the mechanism of reinforcing steel fracture, the diagnosis may be basically focused on the bend of reinforcing steels.

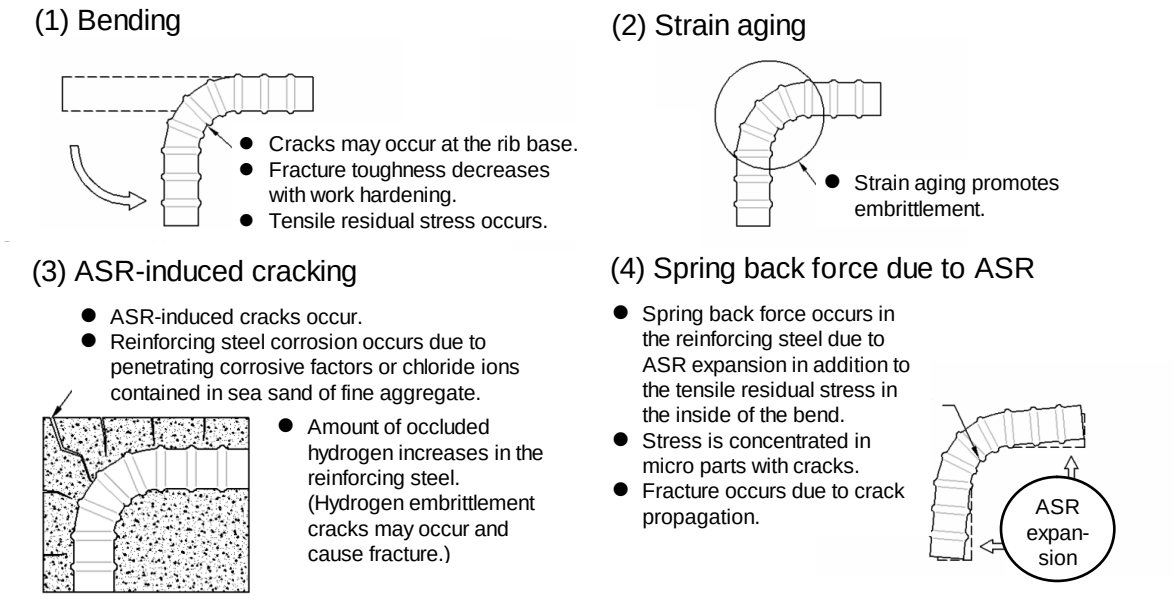

Figure 11. Proposed Mechanism of Reinforcing Steel Fracture

REFERENCES

Japanese Standards Association. (2009). *JIS Handbook: Ferrous Materials & Metallurgy I-2009*, Tokyo, 1951-1953.

Kobayashi, M., Nishikata, A. and Tsuru, T. (2010). "Effect of Stain Rate and Hydrogen Charging Current on Hydrogen Embrittlement of Carbon Steel in High Alkaline Chloride Environment." *zairyo-to-kankyo*, Japan Society of Corrosion Engineering, 59(4), 129-135. (in Japanese)

Matsuyama, S. (1989). *Delayed Fracture*, Nikkan Kogyo Shimbun Ltd., Tokyo. (in Japanese)

Sasaki, K., Hisari, Y., Igarashi, H. and Miyagawa, T. (2008). "Analysis of the stress and strain on bent section of reinforcing bar by finite element method." *Proceedings of Japan Concrete Institute*, JCI, 30(1), 987-992. (in Japanese)

Sasaki, K., Matsumoto, S., Kuzume, K., Kanaumi, S. and Miyagawa, T. (2009). "Expansion Behavior of Prestressed Concrete Beams Deteriorated by Alkali-Silica Reaction in Long Term Exposure Test." *Proceedings of 4th International Conference on Construction Materials: Performance, Innovations and Structural Implications*, JCI, 739-746.

Tarui, T. and Torii, K. (2010). "Fracture Mechanism of Steel Bar by Alkali Silica Reaction." *zairyo-to-kankyo*, Japan Society of Corrosion Engineering, 59(4), 143-150. (in Japanese)

Toyohuku, T., Yoshioka, H. and Yoshimura, Y. (1988). "Actual quality of electric furnace steel bars." *Nihon Doro Kodan Laboratory report*, Nihon Doro Kodan Laboratory, 25, 59-71. (in Japanese)